Noise-aware Quantum Annealing for State Estimation in Power Systems

Quoc-Bao Tran   Thang N. Dinh

Department of Computer Science,
Virginia Commonwealth University, Richmond, VA, USA
tranq3@vcu.edu,   tndinh@vcu.edu

Abstract—**Quantum computing offers potential speedups for power system state estimation, but continuous variables like voltage angles pose challenges for quantum annealers with limited qubit resources. We introduce an iterative quantum annealing approach that progressively narrows the search space for voltage angles in DC power systems. Rather than encoding wide ranges with many qubits, our method uses few-bit encodings with dynamic range refinement across multiple annealing cycles. Testing on IEEE benchmark systems demonstrates that this approach outperforms vanilla encoding of continuous variables while reducing computational resources. This adaptive strategy addresses a fundamental challenge in quantum optimization, mapping continuous variables to discrete quantum bits, and establishes a practical pathway for quantum computing applications in power system operations.**

Index Terms—**state estimation, quantum annealing, QUBO, weighted least squares, quantum computing, power system**

I. INTRODUCTION

Power system state estimation serves as a cornerstone of modern energy management systems, providing critical information for grid operations, security assessment, and market functions. Since its introduction by Schweppe et al. in the early 1970s [1], state estimation has evolved from a theoretical concept to an essential tool implemented in control centers worldwide. The traditional approach formulates state estimation as a weighted least squares (WLS) optimization problem, using redundant supervisory control and data acquisition (SCADA) measurements to compute statistically optimal estimates of network bus voltages. As power grids have become increasingly complex and faced growing cyber-physical security threats, the need for real-time and robust state estimation has become paramount.

Quantum computing offers promising approaches for solving complex optimization problems, many of which can be mapped to Ising models [2], potentially leading to quantum advantage [3]. Recent developments, including Google's Sycamore and Willow processors demonstrating supremacy in a sampling task [4], [5] and D-Wave quantum advantage [6]–[9], indicate progress toward practical quantum applications.

Recent work has explored various quantum computing applications in power systems, including optimal power flow [10], unit commitment [11], and security-constrained economic dispatch [12]. Within state estimation specifically, researchers have investigated PMU placement optimization [13] and distribution system state estimation [14], yet quantum solutions for transmission-level state estimation remain underexplored. Classical approaches have demonstrated fast implementations using belief propagation [15] and hierarchical decomposition methods [16], providing benchmarks against which quantum solutions must compete.

However, current quantum devices face significant constraints that limit their practical application to power system problems. These include a limited number of qubits and connectivity among the qubits, the susceptibility to noise, and finite precision in coefficient representation [17], [18]. Further, state variables such as voltage angles are continuous by nature, requiring discretization for representation in binary form. The conventional approach of wide-range discretization demands high numerical precision, often exceeding what current quantum hardware can reliably support.

To this end, we propose an iterative Quantum Annealing approach for DC power system state estimation, with an emphasis on adaptive range refinement for improved accuracy. Unlike conventional single-stage encodings that attempt to cover the entire solution space at once, our approach progressively narrows the feasible angle domain over multiple iterations by adaptively updating lower and upper bounds based on intermediate solutions. Each iteration employs a modest binary representation and dynamic coefficient scaling to map the WLS problem into a refined QUBO form, which is suitable for efficient processing on D-Wave Quantum Annealing systems.

By narrowing the feasible angle range over multiple annealing rounds, our method addresses the challenges posed by continuous variable encodings and limited qubit precision, while still yielding accuracy that is more robust to noise than single-shot approaches. This iterative refinement allows us to achieve high precision with fewer qubits per variable, making the approach particularly suitable for implementation on current quantum hardware with its inherent limitations.

Experimental validation on IEEE test cases demonstrates consistent convergence and reduced computational overhead compared to static encodings that attempt to achieve the same precision in a single annealing run. For example, our results show that using just 5 bits per angle variable with iterative

refinement can achieve comparable or better accuracy than static approaches using 7 or more bits, reducing the resource requirements for quantum implementation. These findings highlight the potential of quantum computing capabilities for practical power system applications, particularly real-time state estimation in larger power systems where computational efficiency is paramount.

The remainder of this paper is organized as follows. Section II provides background on DC power flow modeling, weighted least squares state estimation, and quantum annealing principles. Section III presents our proposed iterative quantum annealing methodology for power system state estimation. Section IV describes the experimental setup and results on IEEE test cases. Finally, Section V concludes the paper and discusses directions for future research.

a) Related Work: Power system state estimation has undergone significant evolution over five decades. In the 1980s, Monticelli and Garcia [19] developed fast decoupled state estimators, exploiting the weak coupling between real and reactive measurements to accelerate WLS calculations. For robustness against outliers, Mili et al. [20] introduced methods based on least median of squares to improve resilience against multiple bad data points. The 1980s also introduced the idea of distributed (or hierarchical) state estimation to handle growing system sizes and data volumes. Korres [16] proposed distributed multiarea state estimation techniques, while Gómez-Expósito et al. [14] developed multilevel state estimation paradigms for smart grids.

The DC state estimation model simplifies the AC state estimation problem. Schweppe and Rom [1] introduced the concept of approximate models for power system state estimation, establishing the foundation for DC state estimation. Monticelli [21] extended the DC state estimation framework by incorporating circuit breaker modeling. Graven and van Amerongen [22] further developed the DC approach by formulating the state estimation problem within a linear programming framework rather than traditional weighted least squares.

Quantum computing applications to power systems represent an emerging field with significant transformative potential. Ajagekar and You [11] provided a comprehensive overview of quantum computing opportunities for energy systems optimization, identifying both near-term applications and future challenges. Chen and Abur [13] presented methodologies for optimal PMU placement designed to enhance bad data detection capabilities in power system state estimation. Xie et al. [23] developed graph theory-based methodologies for optimal PMU placement and multiarea state estimation that could be formulated as QUBO problems suitable for quantum processing. Feng et al. [10] proposed quantum algorithms for power flow analysis that demonstrated potential computational advantages over classical methods. Zhou et al. [12] explored broader applications of quantum computing across various power system domains, examining both theoretical frameworks and implementation considerations.

Recent research has explored various avenues to tackle real-time state estimation challenges using belief propagation-based methods [15]. Despite the limitations of near-term quantum devices, quantum annealers, particularly D-Wave systems, have shown potential for handling state estimation problems effectively when properly formulated. Current quantum-annealing workflows suffer not only from *limited coefficient precision* but also from the *minor-embedding step*, whose heuristic runtime can dominate end-to-end execution time on D-Wave machines [24]. Greer and O'Malley's subsurface inversion scheme discretises every continuous parameter afresh at each Newton iteration, producing a *new* QUBO each time and therefore forcing the embedding solver to run from scratch; the authors report that embedding often exceeds annealing time for problem sizes beyond 7×7 cells [25]. The recent QESA hybrid of Djidjev also regenerates a QUBO at every macro-step because the binary search-direction vector changes dimension as the algorithm progresses [26]. Even domain-wall/unary encodings, while qubit-efficient for multi-valued integers [27], [28], require a fresh embedding whenever the resolution is altered.

IRR-QA *eliminates this overhead*: each angle is mapped to a *fixed-length* spin binary word and the QUBO connectivity pattern never changes throughout the outer "zoom-in" loop. Consequently, the (costly) minor-embedding is computed *once*, reused in every iteration, and its chain strengths remain valid because all coefficients are rescaled to the same hardware-legal range. This static-topology property directly tackles what is increasingly the dominant bottleneck in large QA workflows, while still delivering the precision gains of iterative range refinement that one-shot encodings cannot match.

II. PRELIMINARIES AND PROBLEM FORMULATION

This section establishes the foundational concepts necessary for understanding our proposed approach, presenting them in a hierarchical structure that connects traditional power system analysis with quantum computing applications.

A. Power System State Estimation Fundamentals

Power system state estimation serves as a critical function in modern energy management systems, providing real-time assessment of system conditions based on imperfect measurements. In its comprehensive form, AC state estimation determines both voltage magnitudes and phase angles across the network by processing measurements such as power flows, injections, and voltage magnitudes. The nonlinear AC power flow equations relate complex bus voltages to power injections through:

$$S_i = V_i \sum_{j=1}^{n} Y_{ij}^* V_j^* = P_i + jQ_i \tag{1}$$

where S_i is the complex power injection at bus i, V_i is the complex voltage at bus i, Y_{ij} is the element of the bus admittance matrix, and P_i and Q_i are the active and reactive power injections, respectively. Figure 1 shows an example of a power system with four buses and lines connecting them. This nonlinear relationship makes AC state estimation computationally intensive, especially for large systems.
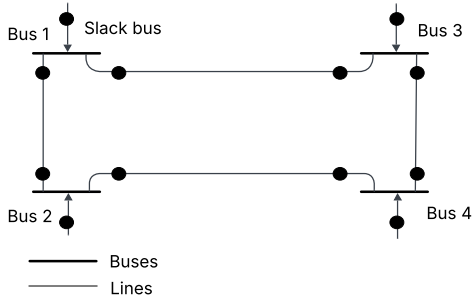
Fig. 1. The Topology of 4-Bus System

The DC state estimation model offers a valuable simplification that maintains analytical utility while significantly reducing computational complexity. This linearized approximation focuses solely on active power and voltage angles, making several key assumptions: negligible resistance compared to reactance, small voltage angle differences, voltage magnitudes approximately equal to 1.0 per unit, and negligible reactive power flows. These simplifications transform the nonlinear AC equations into a linear relationship between power flows and voltage angles, making the problem more tractable for various applications, including quantum computing implementations.

B. DC Power Flow and State Estimation

Under the DC approximation assumptions, the nonlinear AC power flow equations simplify considerably. By assuming voltage magnitudes of 1.0 per unit and small angle differences, the sine of angle differences can be approximated by the angle difference itself, and the cosine term approaches 1. Additionally, by neglecting line resistance compared to reactance, the active power flow P_{ij} from bus i to bus j simplifies to:

$$P_{ij} = \frac{\theta_i - \theta_j}{g_{ij}} = B_{ij}(\theta_i - \theta_j) \quad (2)$$

where θ_i and θ_j are the voltage phase angles at buses i and j, respectively, g_{ij} is the reactance of the line connecting the two buses, and $B_{ij} = \frac{1}{g_{ij}}$ is the susceptance.

The active power injection at bus i is the sum of all power flows from bus i to its connected buses:

$$P_i = \sum_{j \in \Omega_i} P_{ij} = \sum_{j \in \Omega_i} B_{ij}(\theta_i - \theta_j) \quad (3)$$

where Ω_i is the set of all buses connected to bus i.

This can be written in matrix form as:

$$\mathbf{P} = \mathbf{B}\boldsymbol{\theta} \quad (4)$$

where $\mathbf{P}$ is the vector of bus power injections, $\boldsymbol{\theta}$ is the vector of voltage phase angles, and $\mathbf{B}$ is the bus susceptance matrix.

In the DC state estimation framework, measurements ($\mathbf{z}$) relate to state variables ($\mathbf{x}$) through a linear function:

$$\mathbf{z} = \mathbf{Hx} + \mathbf{e} \quad (5)$$

where $\mathbf{H}$ is the measurement Jacobian matrix and $\mathbf{e}$ represents measurement errors. In the DC model, the state vector x corresponds to the bus voltage angles θ, excluding the reference bus. The weighted least squares (WLS) approach seeks to find the state estimate $\hat{\mathbf{x}}$ that minimizes:

$$J(\mathbf{x}) = (\mathbf{z} - \mathbf{Hx})^T \mathbf{R}^{-1}(\mathbf{z} - \mathbf{Hx}) \quad (6)$$

where $\mathbf{R}$ is the measurement error covariance matrix. This can be rewritten in the form:

$$J(\mathbf{x}) = \mathbf{x}^T \mathbf{A}\mathbf{x} + \mathbf{b}^T \mathbf{x} + c \quad (7)$$

with $\mathbf{A} = \mathbf{H}^T \mathbf{R}^{-1} \mathbf{H}$ and $\mathbf{b} = -2\mathbf{H}^T \mathbf{R}^{-1} \mathbf{z}$ ($\mathbf{A}$ is upper triangle). Importantly, this quadratic form aligns naturally with quantum optimization problems, making DC state estimation particularly suitable for quantum computing approaches.

C. Quantum Annealing

Quantum annealing represents a specialized computational paradigm for solving optimization problems by exploiting quantum mechanical effects. D-Wave's quantum annealers implement this approach using superconducting flux qubits governed by a time-dependent Hamiltonian:

$$\mathcal{H}(s) = (1 - s)\mathcal{H}_0 + s\mathcal{H}_P \quad (8)$$

where s transitions from 0 to 1 during the annealing process. The initial Hamiltonian $\mathcal{H}_0 = -\sum_i \sigma_i^x$ creates a superposition of all possible states, while the problem Hamiltonian $\mathcal{H}_P = \sum_i h_i \sigma_i^z + \sum_{i<j} J_{ij} \sigma_i^z \sigma_j^z$ encodes the optimization problem we wish to solve.

The quantum annealing process seeks to find the ground state of this Hamiltonian, which corresponds to the optimal solution of the original problem. This approach is particularly effective for problems that can be formulated as Quadratic Unconstrained Binary Optimization (QUBO) problems or their equivalent Ising models.

The Ising model formulation uses spin variables $s_i \in \{-1, +1\}$ to represent a system's energy:

$$E(\mathbf{s}) = \sum_i h_i s_i + \sum_{i<j} J_{ij} s_i s_j \quad (9)$$

This is mathematically equivalent to a QUBO problem using binary variables $y_i \in \{0, 1\}$ through the transformation $s_i = 2y_i - 1$. This equivalence allows us to map our power system state estimation problem, which naturally takes a quadratic form, onto the quantum annealing hardware.

D. Mapping Power System Problems to Quantum Hardware

Implementing DC state estimation on quantum annealers requires bridging continuous power system variables (state variables $\mathbf{x}$) with the binary nature of quantum bits. This mapping introduces several challenges that significantly impact solution quality.

To encode a continuous state variable $x_i \in [L, U]$ into binary form, where L is the lower bound and R is the upper

bound of the state variable (typically $[-\pi, \pi]$), we typically use a set of binary variables $y_{i,0}, y_{i,1}, \ldots, y_{i,n_b-1}$ as follows:

$$x_i = L + d_i \sum_{j=0}^{n-1} 2^j y_{i,j} \qquad (10)$$

where n_b is the number of binary variables used per angle, $d_i = \frac{U-L}{2^{n_b}}$ represents the resolution of the encoding.

With this encoding, our original quadratic objective function $J(\mathbf{x}) = \mathbf{x}^T \mathbf{A}\mathbf{x} + \mathbf{b}^T \mathbf{x} + c$ transforms into a QUBO problem in terms of binary variables, which can then be solved on quantum annealing hardware.

The precision of this encoding directly relates to the number of bits used for each state variable. The discretization error is bounded by:

$$|x_i - \hat{x}_i| \leq d_i \qquad (11)$$

Higher precision requires more qubits, creating a fundamental tradeoff between accuracy and quantum resource requirements.

E. Challenges for Near-term Quantum Computing

Current quantum annealing implementations face several critical challenges when applied to power system state estimation:

1) **Limited qubit resources:** D-Wave systems have limited logical qubits after accounting for connectivity constraints and embedding overhead [24], restricting the precision of continuous variable representations.
2) **Hardware precision and noise sensitivity:** Quantum annealers support limited coefficient precision and are susceptible to environmental noise [17]. As encoding precision increases, QUBO coefficients span multiple orders of magnitude, with smaller coefficients becoming effectively invisible to the annealer or disproportionately affected by noise.
3) **Dynamic range limitations:** The gap between the largest and smallest coefficients in high-precision encodings frequently exceeds hardware capabilities [10], leading to degraded solution quality rather than improvement when adding more qubits.

These hardware-imposed constraints fundamentally limit the effectiveness of straightforward continuous variable encodings on quantum annealers. Our proposed iterative quantum annealing approach in Section 3 addresses these challenges by progressively refining the feasible domain across multiple annealing cycles, achieving high precision with modest qubit resources.

F. Noise of D-Wave Machine

D-Wave quantum annealers face several noise sources that impact solution fidelity [29]. The actual Hamiltonian solved differs from the intended one:

$$E_\delta^{\text{ising}}(\mathbf{s}) = \sum_{i=1}^{N}(h_i + \delta h_i)s_i + \sum_{i=1}^{N}\sum_{j=i+1}^{N}(J_{i,j} + \delta J_{i,j})s_i s_j$$

where δh_i and $\delta J_{i,j}$ represent parameter errors.

The dominant noise sources for *Integrated Control Errors (ICE)* include *background susceptibility*, *flux noise*, *DAC Quantization*, *physical variations* [29]. Additional error sources include temperature fluctuations (affecting thermal excitations), high-energy photon flux (causing unwanted state transitions), and readout errors ($< 1\%$ infidelity). These noise effects collectively limit the achievable dynamic range and precision, particularly impacting large-scale problems where errors accumulate across many qubits.

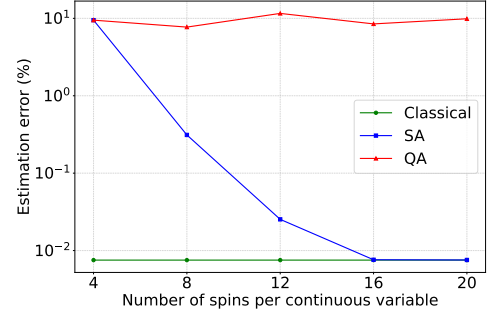## III. ITERATIVE QUANTUM ANNEALING FOR DC POWER SYSTEM STATE ESTIMATION

Fig. 2. Comparison of error results for different numbers of binary variables (n_b) per angle in a 4-bus system

A. Discretizing Continuous Angles into Binary Variables - a Vanilla Approach

We implement the conventional (vanilla) approach that discretizes each state variable x_i using a fixed-range binary encoding through a multi-step process in Section II, D (equation 10). In principle, this approach should yield increasingly accurate results as we allocate more binary variables per state variable. With n_b bits, we can represent 2^{n_b} distinct values across the range $[L_i, U_i]$, giving a theoretical precision of $\frac{U_i - L_i}{2^{n_b}}$. Intuitively, one might expect that increasing the number of qubits would monotonically improve solution quality until reaching some saturation point where additional precision provides diminishing returns.

However, our experiments with the 4-bus test case, illustrated in Figure 2, reveal a more complex reality. Rather than showing consistent improvement with increasing bit count, the error rates exhibit irregular behavior and even deteriorate significantly when using more qubits.

This counterintuitive behavior stems from fundamental limitations in current quantum annealing hardware. The D-Wave quantum annealer requires all QUBO coefficients to fall within a limited dynamic range with finite precision. As we increase the number of bits used in the angle encoding, the corresponding QUBO coefficients span a wider range of magnitudes, many of which become too small relative to the dominant terms. The annealer effectively "rounds off" these small coefficients due to its limited precision, leading to unpredictable behavior and potentially increased errors.

Furthermore, wider coefficient ranges exacerbate the impact of noise in the quantum annealing process. Even minor fluctuations can disproportionately affect smaller coefficients, causing the annealer to misconstrue the optimization landscape. This noise sensitivity increases with the number of bits used in the encoding, explaining the diminished performance observed with higher bit counts.

These observations highlight a fundamental challenge in applying quantum annealing to power system state estimation: we cannot arbitrarily increase precision through brute-force allocation of additional qubits. Instead, we must develop more sophisticated approaches that achieve high accuracy while working within the constraints of current quantum hardware.

B. Iterative Range-Refinement Quantum Annealing (IRR-QA) Overview

Conventional approaches to quantum annealing for continuous optimization problems typically discretize a fixed angle range (e.g., $[-\pi, \pi]$) once and map it onto a quadratic unconstrained binary optimization (QUBO) problem. This technique often requires a high number of qubits to achieve sufficient resolution, especially for large power systems or high-precision applications. To address this challenge, we propose an Iterative Range-Refinement Quantum Annealing (IRR-QA) approach that refines the angle domain over multiple rounds of annealing. By "zooming in" on the most relevant subranges, we decrease the total computational overhead and reduce the number of qubits required to attain a given accuracy.

1) QUBO Mapping and Dynamic Scaling: For the first iteration ($k = 1$), we initialize each state variable's bounds to a reasonable range $L_i^{(1)} = -\pi$ and $U_i^{(1)} = \pi$ for all i, which covers the normal operating range of power system state variables.

In each iteration k, we transform our continuous optimization problem into a QUBO formulation suitable for quantum processing. This transformation requires encoding each continuous state variable $x_i \in [L_i^{(k)}, U_i^{(k)}]$ using n_b binary variables $y_{i,0}, y_{i,1}, \ldots, y_{i,n_b-1}$ according to:

$$x_i = L_i^{(k)} + d_i^{(k)} \sum_{j=0}^{n_b-1} 2^j y_{i,j} \tag{12}$$

where $d_i^{(k)} = \frac{U_i^{(k)} - L_i^{(k)}}{2^{n_b}}$ determines the resolution achievable with n_b bits in the current iteration's range.

Substituting this binary representation into our WLS objective function $J(\mathbf{x}) = \mathbf{x}^T \mathbf{A} \mathbf{x} + \mathbf{b}^T \mathbf{x} + c$:

$$\begin{aligned}
J(\mathbf{y}) = & \sum_{i=1}^{n} \sum_{j=i}^{n} A_{ij} \left(L_i^{(k)} + d_i^{(k)} \sum_{p=0}^{n_b-1} 2^p y_{i,p} \right) \\
& \times \left(L_j^{(k)} + d_j^{(k)} \sum_{q=0}^{n_b-1} 2^q y_{j,q} \right) \\
& + \sum_{i=1}^{n} b_i \left(L_i^{(k)} + d_i^{(k)} \sum_{p=0}^{n_b-1} 2^p y_{i,p} \right) + c
\end{aligned} \tag{13}$$

where n is the number of buses excluding the reference bus. Expanding this expression and collecting terms with the same binary variables yields the QUBO form:

$$\begin{aligned}
J(\mathbf{y}) = & \sum_{i=1}^{n} \sum_{p=0}^{n_b-1} \sum_{j=i}^{n} \sum_{q=0}^{n_b-1} Q_{(i,p),(j,q)} y_{i,p} y_{j,q} \\
& + \sum_{i=1}^{n} \sum_{p=0}^{n_b-1} Q_{(i,p)} y_{i,p} + Q_0
\end{aligned} \tag{14}$$

with the following coefficients:

$$Q_{(i,p),(j,q)} = \begin{cases} A_{ii} d_i^{(k)2} 2^{p+q}, & i = j, \\ 2 A_{ij} d_i^{(k)} d_j^{(k)} 2^{p+q}, & i < j, \end{cases}$$

$$Q_{(i,p)} = d_i^{(k)} 2^p \left(b_i + 2 A_{ii} L_i^{(k)} + 2 \sum_{\substack{j=1 \\ j \neq i}}^{n} A_{ij} L_j^{(k)} \right),$$

$$Q_0 = c + \sum_{i=1}^{n} \left(b_i L_i^{(k)} + A_{ii} L_i^{(k)2} \right) + 2 \sum_{i<j} A_{ij} L_i^{(k)} L_j^{(k)}. \tag{15}$$

The constant term Q_0 does not affect the optimization and can be omitted when solving the QUBO problem.

2) Adaptive Range Update with Boundary Protection: A critical aspect of our approach is the adaptive range update mechanism. After obtaining an estimated state variable $\hat{x}_i^{(k)}$ in iteration k, we update bounds as follows:

$$L_i^{(k+1)} = \hat{x}_i^{(k)} - \delta_i^{(k)} \tag{16}$$

$$U_i^{(k+1)} = \hat{x}_i^{(k)} + \delta_i^{(k)} \tag{17}$$

$$\delta_i^{(k+1)} = \frac{1}{2} \delta_i^{(k)} \tag{18}$$

To handle cases where the estimated state variable is near the boundary of the current range, we implement a boundary protection mechanism:

$$\text{if } |\hat{x}_i^{(k)} - L_i^{(k)}| < \gamma \cdot \delta_i^{(k)} \text{ then } L_i^{(k+1)} = L_i^{(k)} - \delta_i^{(k)}/4 \tag{19}$$

$$\text{if } |U_i^{(k)} - \hat{x}_i^{(k)}| < \gamma \cdot \delta_i^{(k)} \text{ then } U_i^{(k+1)} = U_i^{(k)} + \delta_i^{(k)}/4 \tag{20}$$

where γ is a proximity threshold parameter. This ensures the solution space doesn't prematurely exclude potential optimal regions when an estimate lies near the current boundaries.

Algorithm: Iterative Quantum Annealing for State Estimation with Boundary Protection

---

1: **Input:** WLS matrices $\mathbf{A}, \mathbf{b}$; initial range $\mathbf{L}^{(1)}, \mathbf{U}^{(1)}$; iteration limit K; tolerance ϵ; proximity threshold γ
2: **Output:** Estimated state variables $\hat{\mathbf{x}}$
3: Initialize $\delta_i^{(1)} \leftarrow \frac{U_i^{(1)} - L_i^{(1)}}{2}$ for each state variable i
4: **for** $k = 1$ to K **do**
5:     Build QUBO matrix $\mathbf{Q}^{(k)}$ by:
6:        1) Encoding each $x_i \in [L_i^{(k)}, U_i^{(k)}]$ with n_b bits
7:        2) Mapping WLS cost $(\mathbf{x}^T \mathbf{A} \mathbf{x} + \mathbf{b}^T \mathbf{x})$ into QUBO
8:     Solve QUBO on quantum annealer to get binary solution $\mathbf{y}^{(k)}$
9:     Decode $\mathbf{y}^{(k)} \rightarrow \hat{\mathbf{x}}^{(k)}$ in real domain
10:     **if** $k > 1$ **and** $\|\hat{\mathbf{x}}^{(k)} - \hat{\mathbf{x}}^{(k-1)}\| \leq \epsilon$ **then**
11:        **break**   // Converged
12:     **end if**
13:     Update bounds around each $\hat{x}_i^{(k)}$:
14:        $L_i^{(k+1)} \leftarrow \hat{x}_i^{(k)} - \delta_i^{(k)}$
15:        $U_i^{(k+1)} \leftarrow \hat{x}_i^{(k)} + \delta_i^{(k)}$
16:        // Apply boundary protection mechanism
17:        **if** $|\hat{x}_i^{(k)} - L_i^{(k)}| < \gamma \cdot \delta_i^{(k)}$ **then**
18:           $L_i^{(k+1)} \leftarrow L_i^{(k)} - \delta_i^{(k)}/4$
19:        **end if**
20:        **if** $|U_j^{(k)} - \hat{x}_i^{(k)}| < \gamma \cdot \delta_i^{(k)}$ **then**
21:           $U_i^{(k+1)} \leftarrow U_i^{(k)} + \delta_i^{(k)}/4$
22:        **end if**
23:        $\delta_i^{(k+1)} \leftarrow \frac{1}{2} \delta_i^{(k)}$
24: **end for**
25: **return** $\hat{\mathbf{x}}^{(k)}$

---

3) Complete Algorithm: Our method utilizes an iterative refinement approach with boundary protection to efficiently solve the DC power system state estimation problem. Starting with a relatively wide range for each angle variable and using a modest number of bits (typically 5 bits per variable), we progressively narrow the search space while maintaining numerical stability and solution accuracy.

The algorithm operates on a set of state variables $\mathbf{x} = \{x_1, x_2, \ldots, x_n\}$ (excluding the reference bus), with iteration-specific bounds $\mathbf{L}^{(k)} = \{L_1^{(k)}, \ldots, L_n^{(k)}\}$ and $\mathbf{U}^{(k)} = \{U_1^{(k)}, \ldots, U_n^{(k)}\}$. Initially, these bounds typically span a physically reasonable range such as $[-\pi, \pi]$ radians for each state variable.

A key strength of our approach is the boundary protection mechanism as described in Equations (19)-(20) that prevents premature exclusion of potentially optimal regions. When an estimated state variable $\hat{x}_i^{(k)}$ is too close to its current boundaries (within $\gamma \cdot \delta_i^{(k)}$ distance), we extend the corresponding bound outward rather than simply centering the new interval. This protection mechanism is crucial when the true solution lies near the edge of the current search range.

Otherwise, when the estimated state variable is sufficiently far from the boundaries, we center the new bounds around the current estimate following the standard update rules in Equations (16)-(17). In all cases, we halve the delta value for the next iteration as shown in Equation (18), ensuring exponential convergence under ideal conditions.

The algorithm also employs dynamic scaling of QUBO

coefficients to address hardware precision limitations as the feasible range narrows. The combination of boundary protection and coefficient scaling makes our approach well-suited for implementation on current quantum annealing devices with inherent hardware limitations.

The algorithm terminates either when reaching a predefined maximum number of iterations K or when the solution converges, indicated by minimal change between successive estimates (i.e., $\|\hat{\mathbf{x}}^{(k)} - \hat{\mathbf{x}}^{(k-1)}\| \leq \epsilon$ for some small tolerance ϵ). This convergence criterion can be formalized as:

$$\|\hat{\mathbf{x}}^{(k)} - \hat{\mathbf{x}}^{(k-1)}\|_2 = \sqrt{\sum_i (\hat{x}_i^{(k)} - \hat{x}_i^{(k-1)})^2} \leq \epsilon \qquad (21)$$

In practice, we find that 5-10 iterations are typically sufficient to achieve convergence as defined in Equation (21) for moderately sized power systems.

This adaptive "zoom-in" procedure substantially reduces the feasible space with each iteration, allowing more accurate solutions with the same number of qubits. The combination of smaller intervals and dynamic coefficient scaling also reduces numerical precision issues on quantum hardware, making the approach particularly well-suited for implementation on current and near-term quantum annealing devices with their inherent hardware limitations. Our experimental results, presented in Section IV, demonstrate that this approach can achieve solution quality comparable to classical methods while using substantially fewer qubits than would be required in a single-stage quantum approach.

IV. NUMERICAL EXPERIMENTS

A. Evaluation Methodology

To evaluate estimation accuracy, we employ the Sum of Absolute Residuals (Normalized), computed as

$$\text{SumError}_{\text{method}} = \frac{\sum_{i=1}^{m} |z_i - z_{i,\text{method}}|}{\sum_{i=1}^{m} |z_i|},$$

where z_i represents the true measurement and $z_{i,\text{method}}$ denotes the estimated measurement from each method. This metric normalizes performance across different system sizes and measurement scales, enabling direct comparison between methods regardless of the magnitude of the original measurements. A lower SumError value indicates higher accuracy and better estimation performance.

We evaluate our approach on two standard power network topologies: a 4-bus system adapted from [11] and the IEEE 5-bus test case. Each bus has active power injection measurements, while selected lines have power flow measurements. For both systems, we designate one bus as the reference (angle set to zero) and estimate the remaining bus voltage angles. The datasets include redundant measurements with a redundancy ratio of approximately 2.0, mimicking typical SCADA configurations in real-world power systems. Figure 1 illustrates our 4-bus system. Bus 1 is designated as the slack (reference) bus, providing the voltage reference and balancing power in the network. The transmission network

consists of four primary lines: one connecting Bus 1 to Bus 2 (vertically), another connecting Bus 3 to Bus 4 (vertically), and two horizontal lines connecting Bus 1 to Bus 3 and Bus 2 to Bus 4, respectively.

We compare three approaches in our evaluation: Classical Weighted Least Squares (WLS) using Singular Value Decomposition, Simulated Annealing (SA) with discretized angles, and our proposed Iterative Range-Refinement Quantum Annealing (IRR-QA). We also implemented a non-iterative quantum annealing approach with fixed angle ranges to establish a baseline and demonstrate the advantages of our iterative refinement strategy.

TABLE I
ABSOLUTE RESIDUAL COMPARISON FOR THE 4-BUS SYSTEM

Measure	Actual	Classical	SA	QA	IRR-QA
Bus1 injection	−4.940	0.143	0.389	1.512	0.271
Bus2 injection	−2.754	0.244	0.039	5.980	0.061
Bus3 injection	6.230	0.257	0.481	3.004	0.630
Bus4 injection	2.970	0.863	0.597	2.970	0.666
Flow1→2	−0.252	0.046	0.277	2.974	0.280
Flow1→3	−4.693	0.091	0.107	1.467	0.014
Flow2→4	−3.015	0.282	0.307	3.015	0.210
Flow3→4	1.502	0.313	0.553	1.502	0.581
Flow2→1	0.253	0.045	0.276	2.973	0.279
Flow3→1	4.751	0.033	0.049	1.525	0.072
Flow4→2	2.970	0.327	0.352	2.970	0.255
Flow4→3	−1.493	0.304	0.544	1.493	0.572

TABLE II
ABSOLUTE RESIDUAL COMPARISON FOR THE IEEE 5-BUS SYSTEM

Measure	Actual	Classical	SA	QA	IRR-QA
Bus1 injection	0.085	0.000	0.015	0.219	0.005
Bus2 injection	−3.658	0.000	0.089	1.687	0.138
Bus3 injection	4.949	0.002	0.103	1.099	0.238
Bus4 injection	−1.899	0.000	0.130	1.775	0.151
Bus5 injection	0.524	0.000	0.046	0.793	0.232
Flow1→2	0.837	0.001	0.015	0.299	0.016
Flow1→3	−0.837	0.000	0.016	0.299	0.016
Flow2→3	−0.752	0.000	0.000	0.080	0.011
Flow2→4	0.751	0.000	0.001	0.079	0.011
Flow2→5	−1.282	0.002	0.004	0.207	0.019
Flow3→4	1.279	0.002	0.008	0.203	0.023
Flow4→5	−0.795	0.000	0.024	0.437	0.014
Flow2→1	0.793	0.001	0.026	0.435	0.013
Flow3→1	−0.747	0.000	0.043	0.747	0.161
Flow3→2	0.746	0.001	0.043	0.746	0.161
Flow4→2	2.915	0.001	0.107	1.386	0.208
Flow5→2	−2.915	0.001	0.107	1.386	0.208
Flow4→3	0.222	0.001	0.003	0.047	0.071
Flow5→4	−0.222	0.000	0.003	0.047	0.071

B. Hardware and Parameter Settings

All quantum annealing experiments were conducted on the D-Wave *Advantage_system6.4* Quantum Processing Unit with the Pegasus topology and 5,640 physical qubits. We used an annealing time of 20 microseconds with 1000 reads per annealing cycle. The chain strength was automatically calculated based on problem coefficients to balance embedding stability against solution quality. Minor embeddings were generated using *minorminer* [24], translating our logical problem

TABLE III
RESULTS FOR 4-BUS DC STATE ESTIMATION

Method	Bits/Angle	Iterations	SumError (Normalized)
Classical WLS	N/A	N/A	0.08
Simulated Annealing	5	10	0.11
QA	5	N/A	**1.01**
IRR-QA	5	10	**0.11**

TABLE IV
RESULTS FOR IEEE 5-BUS DC STATE ESTIMATION

Method	Bits/Angle	Iterations	SumError (Normalized)
Classical WLS	N/A	N/A	0.0005
Simulated Annealing	5	10	0.0299
QA	5	N/A	**0.4568**
IRR-QA	5	10	**0.0674**

formulation into the physical qubit layout of the quantum processor. During execution, we encountered chain breaks in approximately 15-20% of reads for the 4-bus system, which were handled through majority voting during post-processing.

For the IRR-QA approach, we selected 5 bits per angle based on empirical testing, with initial angle bounds of $[-\pi, \pi]$ radians. We set a maximum of 10 iterations with early stopping when convergence was detected using a tolerance threshold of $\epsilon = 10^{-3}$. The range reduction factor was set to 2.0, effectively halving the search range after each iteration. These parameters were selected to balance precision requirements against quantum hardware constraints identified in Section 2.5.

C. Data Generation Process

The data for Figures 2, 3, 5, and 4 was generated using a synthetic test framework that creates realistic power system state estimation scenarios. The implementation uses a bus-

TABLE V
EXECUTION TIMES FOR IEEE 5-BUS DC STATE ESTIMATION

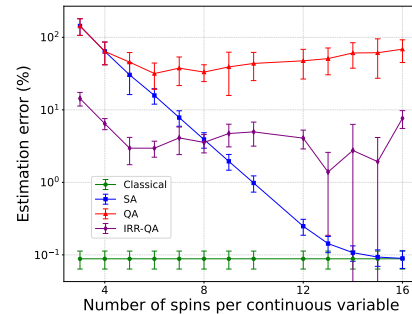| Method	Running Time
SVD (Classical)	0.028498
Simulated Annealing	6.957651
IRR-QA	1.175155
IRR-QA (re-used embedding)	1.478685

Fig. 3. Comparing the sum of errors for different numbers of spins per angle in a 4-bus system
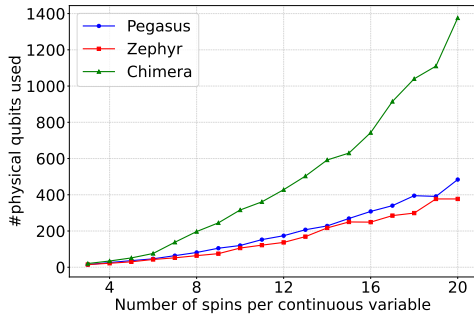
Fig. 4. Comparing the number of physical qubits used for different numbers of spins per angle in a 4-bus system on three DWave machine generations: Chimera, Pegasus, Zephyr
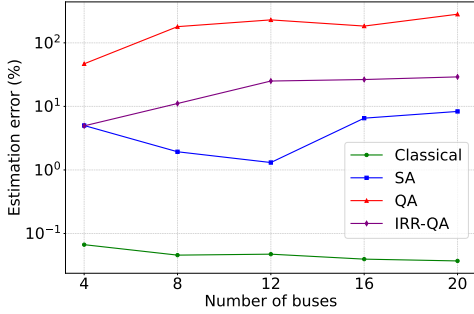

Fig. 5. Comparing the sum of errors for 8 spins per angle with SA, QA, and 5 spins per angle with IRR-QA in different bus systems
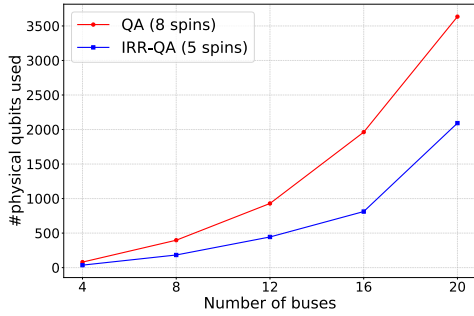

Fig. 6. Comparing the number of physical qubits used for 8 spins per angle with QA and 5 spins with IRR-QA on the Pegasus machine in different bus systems
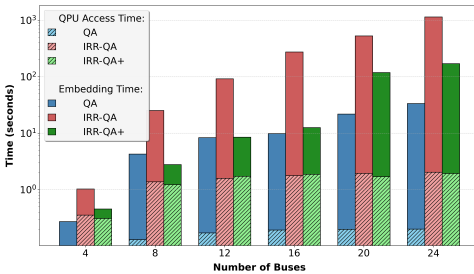

Fig. 7. QPU access time and embedding overhead time comparison

based network model with controlled parameters, where "true" bus voltage angles are constrained to 6-bit binary fractions for precise benchmarking. For each test case, the framework generates power injection measurements for all buses and branch flow measurements between connected buses, with con-figurable Gaussian noise (0.01 standard deviation) to simulate real-world measurement errors. This controlled environment allows for systematic comparison of different state estimation approaches (Classical WLS, Simulated Annealing, Quantum Annealing, and IRR-QA) across varying numbers of qubits per variable.

D. Results and Analysis

Fig. 3 demonstrates the relationship between estimation error and the number of qubits per variable for a 4-bus system. Notably, standard quantum annealing with fixed ranges shows non-improved or degraded performance when using more than 6 qubits per variable. This counterintuitive result confirms the hardware precision and noise challenges discussed earlier, where higher bit precision produces worse results due to the increased range of coefficient magnitudes exceeding the effective precision of the quantum hardware. Our IRR-QA approach produces the smallest sum error up to 8 spins per variable, outperforming both the simulated annealing (SA) and the vanilla quantum annealing (QA) approaches (except for the classical one). For more than 8 spins per variable, even IRR-QA starts to degrade in quality with no clear improvement in solution quality.

As illustrated in Fig. 5 and Fig. 6, our IRR-QA approach demonstrates significant advantages over standard QA implementations across varying power system sizes. Fig. 5 presents estimation errors on a logarithmic scale, demonstrating the relative performance of each approach. While classical methods maintain superior accuracy (below 0.1%) across all system sizes, IRR-QA significantly outperforms standard QA, keeping errors between 5-30% compared to QA's 40-300% error rates. Fig. 6 reveals that physical qubit requirements increase quadratically with system size for both methods, but IRR-QA consistently requires approximately 40% fewer qubits than standard QA. For a 20-bus system, standard QA with 8 spins per angle demands nearly 3,600 physical qubits, while IRR-QA achieves better results using only 2,100 qubits with 5 spins per angle.

These results collectively demonstrate that IRR-QA offers a compelling trade-off between quantum resource efficiency and solution accuracy, particularly for larger power systems where standard QA approaches become both resource-intensive and increasingly inaccurate. The substantial reduction in qubit requirements makes our approach more feasible for implementation on near-term quantum hardware with limited qubit connectivity and coherence times.

Table III presents the performance metrics for the 4-bus system, averaged over 10 independent runs. The classical WLS solution achieves the lowest error (0.0822), as expected for this small-scale problem with a well-conditioned linear model. Our IRR-QA approach produces a normalized error of 0.1086. The

physical qubit requirement for the IRR-QA implementation was 37 qubits after embedding, with an average chain length of 2.5 physical qubits per logical qubit. The solution typically converged within 4-6 iterations, with diminishing improvements in subsequent iterations.

For the IEEE 5-bus system, summarized in Table IV, the performance gap between classical and quantum methods widens. Classical WLS achieves remarkably low error (0.0005), demonstrating its effectiveness for small, well-posed problems. The IRR-QA approach (0.0674) shows a higher error than simulated annealing (0.0299) in this case.

Fig. 4 demonstrates the number of physical qubits used for different numbers of spins per angle in a 4-bus system across three D-Wave machine generations: Chimera [30], Pegasus [31], and Zephyr [32]. These generations represent the evolution of D-Wave's quantum annealer architectures with progressively improved qubit connectivity and reduced embedding overhead. The graph reveals a concerning significant growth in physical qubit requirements as we increase encoding precision, with the older Chimera architecture requiring nearly 1,400 physical qubits for just 20 bits per variable - an extraordinary overhead compared to the mere 3 continuous variables being modeled. Even with the architectural improvements in Pegasus and Zephyr, which reduce this overhead significantly, the resource requirements still scale almost linearly, demanding over 400 physical qubits for 20 bits per variable. This substantial qubit inefficiency, combined with the solution quality degradation shown in Fig. 3, provides compelling evidence for our IRR-QA approach, which achieves better accuracy using only 5 bits per variable (approximately 37 physical qubits). By iteratively refining the angle ranges, IRR-QA effectively mitigates the resource overhead that plagues conventional quantum annealing implementations.

Fig. 7 illustrates the performance comparison of QA, IRR-QA, and IRR-QA+ methods across varying numbers of buses with $n_b = 5$, showing both embedding time (solid bars) and QPU access time (hatched bars) on a logarithmic scale. The results reveal that IRR-QA+ achieves approximately the same total execution time as standard QA, despite requiring multiple iterations. This efficiency is achieved through IRR-QA+'s fixed embedding strategy, which reuses the same embedding across all iterations and eliminates the need to recompute embeddings as QUBO coefficients are rescaled within the same connectivity pattern. In contrast, IRR-QA demonstrates significantly higher execution times due to the embedding overhead incurred at each iteration. IRR-QA+ achieves logarithmic time savings compared to IRR-QA, making the iterative approach practically viable. The embedding time dominates the total execution time for all methods, particularly as system size increases, while QPU access times (shown as hatched portions) remain relatively small and consistent across approaches.

Detailed examination of per-measurement errors reveals systematic patterns in the performance of our IRR-QA approach. Power flow measurements between adjacent buses consistently show lower estimation errors compared to power injection measurements that depend on multiple angle variables simul-taneously. This pattern emerges because power flow measurements create a more direct relationship between variables and measurements, making them less susceptible to the cumulative effects of embedding and discretization errors. Tables I and II provide comprehensive measurement-by-measurement error comparisons, revealing that while the normalized error metric provides a clear overall picture, some individual measurements with small absolute values show larger relative errors.

E. Discussion

Our experiments demonstrate that using 5 bits per angle with iterative refinement provides an effective balance between accuracy and qubit requirements for DC power system state estimation. Attempts to increase precision through additional bits in standard quantum annealing actually degraded performance due to hardware precision limitations and increased noise sensitivity, confirming the theoretical challenges outlined in Section 2.5. For the 4-bus system, the IRR-QA approach required 37 physical qubits while achieving comparable accuracy to methods that would theoretically require higher bit precision. This resource efficiency represents a practical advantage for implementation on current quantum hardware with limited qubit connectivity and precision.

Several limitations of our current evaluation should be addressed in future work. Testing on larger power systems is needed to fully validate the scalability benefits suggested by our initial results. While our iterative approach shows resilience to quantum hardware noise, systematic testing with controlled noise levels would provide stronger evidence of its robustness. The current evaluation does not include scenarios with bad measurements, which are common in practical power system operation and represent an important challenge for any state estimation method. Additionally, all tests were performed on static system snapshots rather than time-series data that would better represent evolving system conditions. Future research should explore these aspects, along with more sophisticated embedding techniques that could reduce physical qubit requirements and enhance solution quality, potentially incorporating dynamic qubit compression approaches [33].

In summary, our IRR-QA approach demonstrates promising performance for DC power system state estimation, particularly in terms of computational efficiency and qubit resource utilization. While classical methods remain superior for small systems where matrix operations can be performed efficiently, the iterative refinement strategy effectively addresses key challenges in quantum implementations and establishes a foundation for applying quantum computing to larger power system optimization problems as hardware capabilities continue to advance.

V. CONCLUSION

This paper presents an iterative range-refinement quantum annealing (IRR-QA) approach for DC power system state estimation that addresses hardware limitations in current quantum annealers. The method progressively narrows the search space for voltage angles across multiple annealing cycles,

using fixed-length binary encodings with dynamic range updates. Experimental validation on IEEE 4-bus and 5-bus test cases shows that IRR-QA achieves comparable accuracy to simulated annealing while using 40% fewer physical qubits than conventional quantum annealing approaches. The method converges within 4-6 iterations using 5 bits per angle variable, requiring 37 physical qubits for the 4-bus system compared to over 400 qubits needed for equivalent precision in single-stage approaches.

The static QUBO connectivity pattern eliminates embedding overhead across iterations, resulting in execution times comparable to standard quantum annealing despite the iterative nature. However, performance gaps remain between quantum methods and classical WLS, particularly for well-conditioned small systems where classical approaches achieve sub-1% errors.

Future work will evaluate scalability on larger power systems, incorporate bad data detection capabilities, and investigate hybrid classical-quantum approaches that leverage the strengths of both paradigms for practical power system applications.

<div align="center">REFERENCES</div>

[1] F. C. Schweppe and D. B. Rom, "Power system static-state estimation, part ii: Approximate model," *IEEE Transactions on Power Apparatus and Systems*, no. 1, pp. 125–130, 1970.

[2] A. Lucas, "Ising formulations of many np problems," *Frontiers in physics*, p. 5, 2014.

[3] J. Preskill, "Quantum computing in the NISQ era and beyond," *Quantum*, vol. 2, p. 79, aug 2018.

[4] F. Arute, K. Arya, R. Babbush, D. Bacon, J. C. Bardin, R. Barends, R. Biswas, S. Boixo, F. G. Brandao, D. A. Buell *et al.*, "Quantum supremacy using a programmable superconducting processor," *Nature*, vol. 574, no. 7779, pp. 505–510, 2019.

[5] R. Acharya, L. Aghababaie-Beni, I. Aleiner, T. I. Andersen, M. Ansmann, F. Arute, K. Arya, A. Asfaw, N. Astrakhantsev, J. Atalaya *et al.*, "Quantum error correction below the surface code threshold," *arXiv preprint arXiv:2408.13687*, 2024.

[6] A. D. King, J. Raymond, T. Lanting, S. V. Isakov, M. Mohseni, G. Poulin-Lamarre, S. Ejtemaee, W. Bernoudy, I. Ozfidan, A. Y. Smirnov *et al.*, "Scaling advantage over path-integral monte carlo in quantum simulation of geometrically frustrated magnets," *Nature com.*, vol. 12, no. 1, p. 1113, 2021.

[7] B. Tasseff, T. Albash, Z. Morrell, M. Vuffray, A. Y. Lokhov, S. Misra, and C. Coffrin, "On the Emerging Potential of Quantum Annealing Hardware for Combinatorial Optimization," 2022, arXiv:2210.04291.

[8] ——, "On the emerging potential of quantum annealing hardware for combinatorial optimization," *Journal of Heuristics*, pp. 1–34, 2024.

[9] A. D. King, A. Nocera, M. M. Rams, J. Dziarmaga, R. Wiersema, W. Bernoudy, J. Raymond, N. Kaushal, N. Heinsdorf, R. Harris, K. Boothby, F. Altomare, A. J. Berkley, M. Boschnak, K. Chern, H. Christiani, S. Cibere, J. Connor, M. H. Dehn, R. Deshpande, S. Ejtemaee, P. Farré, K. Hamer, E. Hoskinson, S. Huang, M. W. Johnson, S. Kortas, E. Ladizinsky, T. Lai, T. Lanting, R. Li, A. J. R. MacDonald, G. Marsden, C. C. McGeoch, R. Molavi, R. Neufeld, M. Norouzpour, T. Oh, J. Pasvolsky, P. Poitras, G. Poulin-Lamarre, T. Prescott, M. Reis, C. Rich, M. Samani, B. Sheldan, A. Smirnov, E. Sterpka, B. T. Clavera, N. Tsai, M. Volkmann, A. Whiticar, J. D. Whittaker, W. Wilkinson, J. Yao, T. J. Yi, A. W. Sandvik, G. Alvarez, R. G. Melko, J. Carrasquilla, M. Franz, and M. H. Amin, "Computational supremacy in quantum simulation," 2024.

[10] F. Feng, Y. Zhou, and P. Zhang, "Quantum power flow," *IEEE Transactions on Power Systems*, vol. 36, no. 4, pp. 3810–3812, 2021.

[11] A. Ajagekar and F. You, "Quantum computing for energy systems optimization: Challenges and opportunities," *Energy*, vol. 179, pp. 76–89, 2019.

[12] Y. Zhou, Z. Tang, N. Nikmehr, P. Babahajiani, F. Feng, T.-C. Wei, H. Zheng, and P. Zhang, "Quantum computing in power systems," *IEnergy*, vol. 1, no. 2, pp. 170–187, 2022.

[13] J. Chen and A. Abur, "Placement of pmus to enable bad data detection in state estimation," *IEEE Transactions on Power Systems*, vol. 21, no. 4, pp. 1608–1615, 2006.

[14] A. Gomez-Exposito, A. Abur, A. de la Villa Jaen, and C. Gomez-Quiles, "A multilevel state estimation paradigm for smart grids," *Proceedings of the IEEE*, vol. 99, no. 6, pp. 952–976, 2011.

[15] M. Cosovic and D. Vukobratovic, "Fast real-time dc state estimation in electric power systems using belief propagation," in *2017 IEEE International Conference on Smart Grid Communications (SmartGridComm)*. IEEE, 2017, pp. 207–212.

[16] G. N. Korres, "A distributed multiarea state estimation," *IEEE Transactions on Power Systems*, vol. 26, no. 1, pp. 73–84, 2010.

[17] E. Pelofske, "Comparing three generations of d-wave quantum annealers for minor embedded combinatorial optimization problems," *Quantum Science and Technology*, 2023.

[18] K. Boothby, P. Bunyk, J. Raymond, and A. Roy, "Next-Generation Topology of D-Wave Quantum Processors," 2020, arXiv:2003.00133.

[19] A. Monticelli and A. Monticelli, "Fast decoupled state estimator," *State Estimation in Electric Power Systems: A Generalized Approach*, pp. 313–342, 1999.

[20] L. Mili, M. G. Cheniae, and P. J. Rousseeuw, "Robust state estimation of electric power systems," *IEEE Transactions on Circuits and Systems I: Fundamental Theory and Applications*, vol. 41, no. 5, pp. 349–358, 1994.

[21] A. Monticelli, "Modeling circuit breakers in weighted least squares state estimation," *IEEE Transactions on Power Systems*, vol. 8, no. 3, pp. 1143–1149, 1993.

[22] J. Graven and R. van Amerongen, "Static state estimation with dc models and linear programming," *International Journal of Electrical Power & Energy Systems*, vol. 8, no. 4, pp. 241–247, 1986.

[23] N. Xie, F. Torelli, E. Bompard, and A. Vaccaro, "A graph theory based methodology for optimal pmus placement and multiarea power system state estimation," *Electric Power Systems Research*, vol. 119, pp. 25–33, 2015.

[24] J. Cai, W. G. Macready, and A. Roy, "A practical heuristic for finding graph minors," *arXiv preprint arXiv:1406.2741*, 2014.

[25] S. Y. Greer and D. O'Malley, "Early steps toward practical subsurface computations with quantum computing," *Frontiers in Computer Science*, vol. 5, p. 1235784, 2023.

[26] H. N. Djidjev, "Extending quantum annealing to continuous domains: A hybrid method for quadratic programming," 2025, arXiv:2504.02073.

[27] J. Chen, T. Stollenwerk, and N. Chancellor, "Performance of domain-wall encoding for quantum annealing," *IEEE Transactions on Quantum Engineering*, vol. 2, pp. 1–14, 2021.

[28] J. Berwald, N. Chancellor, and R. Dridi, "Understanding domain-wall encoding theoretically and experimentally," 2021, arXiv:2108.12004.

[29] D-Wave Systems Inc., "Errors and error correction," https://docs.dwavequantum.com/en/latest/quantum_research/errors.html, 2024, accessed: 2025-07-17.

[30] P. I. Bunyk, E. M. Hoskinson, M. W. Johnson, E. Tolkacheva, F. Altomare, A. J. Berkley, R. Harris, J. P. Hilton, T. Lanting, A. J. Przybysz *et al.*, "Architectural considerations in the design of a superconducting quantum annealing processor," *IEEE Transactions on Applied Superconductivity*, vol. 24, no. 4, pp. 1–10, 2014.

[31] K. Boothby, P. Bunyk, J. Raymond, and A. Roy, "Next-generation topology of d-wave quantum processors," *arXiv preprint arXiv:2003.00133*, 2020.

[32] K. Boothby, A. D. King, and J. Raymond, "Zephyr topology of d-wave quantum processors," *D-wave technical report series*, 2021.

[33] C. Tran, Q.-B. Tran, H. T. Son, and T. N. Dinh, "Scalable quantum-inspired optimization through dynamic qubit compression," in *Proceedings of the AAAI Conference on Artificial Intelligence*, vol. 39, no. 11, 2025, pp. 11353–11361.